IEEE Access
Multidisciplinary | Rapid Review | Open Access Journal

Received August 2, 2018, accepted October 6, 2018, date of publication October 12, 2018,
date of current version December 18, 2018.

Digital Object Identifier 10.1109/ACCESS.2018.2875854

A Resilient Power System Operation Strategy Considering Transmission Line Attacks

KEXING LAI[1,2], (Student Member, IEEE), YISHEN WANG[1], (Member, IEEE), DI SHI, (Senior Member, IEEE), MAHESH S. ILLINDALA[2], (Senior Member, IEEE), XIAOHU ZHANG[1], (Member, IEEE), AND ZHIWEI WANG[1], (Senior Member, IEEE)

[1]GEIRI North America, San Jose, CA 95134, USA
[2]Department of Electrical and Computer Engineering, The Ohio State University, Columbus, OH 43210, USA

Corresponding author: Di Shi (di.shi@geirina.net)

This work was supported by the SGCC Science and Technology Program through the project Hybrid Energy Storage Management Platform for Integrated Energy System.

ABSTRACT Due to significant losses caused by attacks on power grids, mitigation of transmission line attacks has drawn increasing attention in recent years. It is crucial to develop solutions to mitigate these potential damages. Therefore, this paper presents a novel operational strategy aimed at minimizing unserved energy under the worst case attack on transmission lines of a power system with generators and utility-scale battery energy storage systems. This paper formulates a tri-level optimization problem to model interactions between the operator and the attacker. The upper-level problem represents normal operational actions to hedge against potential attacks and minimize operating costs. Then, the middle-level problem determines the attack strategy, including both attack time and lines to be attacked, to maximize impacts to the grid. The lower-level problem models actions of operators during restoration process by minimizing unserved energy. A column-and-constraint generation method is applied to solve the problem. Numerical case studies are conducted to demonstrate advantages of the proposed model in unserved energy reduction under the worst case transmission line attack.

INDEX TERMS Optimal power flow, power system operation, tri-level optimization, transmission system attack, robust optimization, resilience.

NOMENCLATURE

Sets and indices

T	Set of time periods, index by t
N	Set of buses, index by n
L	Set of transmission lines, index by l
K	Set of iteration numbers, index by k
I	Set of generators, index by i
B	Set of battery energy storage system (BESS), index by b
$D(l)/O(l)$	Indices of destination/origin buses of line l
$I(n)/E(n)$	Inject/extract lines connected to bus n
Ω_b^N	Set of buses connected by BESS b
Ω_n^B	Set of BESSs connected to bus n
Ω_i^N	Set of buses connected by generator i
Ω_n^I	Set of generators connected to bus n

Variables

$Pc_{i,t}$	Power output of generator i at time t during restoration
$Pdc_{b,t}/Pcc_{b,t}$	Discharge/charge power of BESS b at time t during restoration
$RCc_{b,t}$	Stored energy of BESS b at time t during restoration
$Pfc_{l,t}$	Power flow on the line l at time t during restoration
$\theta c_{n,t}$	Voltage phase angle at bus n at time t during restoration
$Lshc_{n,t}$	Load shedding on bus n at time t during restoration
a_l	Binary variable for attack status of the line l. This variable is equal to 1 if attacking and 0 otherwise.
x_t	Binary variable for system status at time t. This variable is equal to 1 during restoration and 0 during normal operation

y_t	Binary variable for start indicator of the restoration at the time t. This variable is equal to 1 if restoration starts at time t and 0 otherwise.
z_t	Binary variable for end indicator of the restoration at the time t. This variable is equal to 1 if restoration ends at time t and 0 otherwise.
$P_{i,t}$	Power output of generator i at time t during normal operation
$Pd_{b,t}/Pc_{b,t}$	Discharge/charge power of BESS on bus n at time t during normal operation
$RC_{b,t}$	Stored energy of BESS on bus n at time t during normal operation
$Pf_{l,t}$	Power flow on the line l at time t during normal operation
$\theta_{n,t}$	Voltage phase angle of bus n at time t during normal operation
$FC_{i,t}$	Fuel cost of generator i at time t
O	An ancillary variable for Bender's decomposition
$\boldsymbol{D}$	Set of dual variables of the lower level problem
$\boldsymbol{M/S}$	Set of primal variables of the upper/lower level problem

Parameters

AD	Duration of restoration process
EB_b	Energy Capacity of installed BESS at bus n
PB_b	Power rating of installed BESS at bus n
$SoC^{\min}$	Minimal value of state-of-charge (SoC)
$SoC^{\max}$	Maximal value of state-of-charge (SoC)
ηb	Efficiency of BESS
w	Weight factor for BESS operating cost
$P_i^{\max}$	Maximal power output of generator i
RU_i	Ramping-up limit of generator i
RD_i	Ramping-down limit of generator i
$Pf_l^{\max}$	Maximal power flow on line l
B_l	Susceptance of line l
$A^{\max}$	Maximal number of concurrent attacks
$Lo_{n,t}$	Demand level at bus n at time t
$voll$	Value of lost loads
$Lo_{n,t}$	Demand level at bus n at time t
CT	Convergence tolerance
$\bar{M}$	A sufficiently large number
a_i, b_i, c_i	Fuel cost coefficients of generator
$f(.)$	Piecewise linearization function
$\boldsymbol{A_u\ B_u\ C_u\ D_u}$	Matrices of constraint coefficients in the upper level problem
$\boldsymbol{A_l\ B_l\ C_l\ D_l}$	Matrices of constraint coefficients in the lower level problem
$\boldsymbol{C/G}$	Vector of coefficients in the objective function of the upper/lower level problem

I. INTRODUCTION

Secure and reliable delivery of electricity to energy consumers is absolutely essential to the economic growth of every nation. Any large and unplanned outages caused by damages to the electric grid infrastructure could have a detrimental effect on the economy. Recent events across the globe reiterate that it is critical to build resiliency of the power grid to malicious attacks on certain transmission or generation components. For instance, the Ukraine power grid experienced multiple cyber-attacks in the recent past [1]. In particular, during the 2015 attack on the Ukraine's grid, up to 73 MWh electricity was impacted. During another instance, in California 2013, about 17 transformers were damaged in Meltcalf substation by malicious elements, thereby causing $15M loss to the downstream customers [2]. In 2003, a transmission line attack in Denmark interrupted the electricity supply to over 5 million customers [3]. In the same year, another country of Georgia was affected by attacks on their transmission towers [3].

In the United States, both lawmakers and federal agencies agree on the necessity and importance to build and operate the power grid against malicious attacks. In 2014, the ranking member of U.S. House Energy and Commerce Committee flagged the electricity power grid as ''not adequately protected'' from either physical or cyber-attacks [3]. The U.S. Department of Energy released a report [4] on how the Western Area Power Administration ''had not always established adequate physical security measures and practices for its critical assets.'' Therefore, the most pressing need is to enhance the power system resilience against attacks through proper scheduling.

Several prior publications had earlier investigated the various types of contingencies [5] caused by malicious attacks on system operations. For instance, Arroyo [6] proposed a bi-level optimization model to analyze the power system vulnerability under attack contingencies. The lower-level problem represents the pursuit of system operator to minimize the load curtailment, and the upper-level optimization problem determines a set of outages. Kim *et al.* [7] used AC power flow equations to identify the most disruptive physical attack that resulted in the largest voltage deviation and load shedding. Based on vulnerability analysis, many researchers conducted studies on reducing the load shedding during restoration from the viewpoints of both planning and operation.

From a planning standpoint, the defense-attack-defense (DAD) model was proposed in [8]–[10] to determine the optimal defending resource allocation for transmission lines with the aim of minimizing unmet demand with attacks under the worst-case scenario. Xiang and Wang [11] considered the uncertainty of attack budget to determine the optimal allocation of defending resources. In [12], mitigating effects of attacks was considered in coordinated generation and transmission expansion, while Moreira *et al.* [13] further discussed renewable energy resources expansion considering potential attacks using the DAD model. From the operational

standpoint, the transmission line switching scheme and other dispatch strategies were considered for system operators to minimize the load shedding under attacks on transmission lines [14]. In [15], the security-constrained optimal power flow has been used to enhance system resilience by incorporating the attack risks. Moreira *et al.* [16] proposed to use the adjustable robust optimization approach for energy and reserve scheduling to minimize cost while encountering transmission contingencies. The existing DAD models for attacks on transmission lines fail to accurately represent and model the variability in attacks, such as choosing the attacking times by considering system restoration durations. They assume that either the components under attack remain unavailable for the entire time interval under consideration, or the attacks can be launched at few specific time instants. Such over-simplified assumptions limit the practicability of proposed solutions. In contrast, this paper proposes a comprehensive model to identify the worst attack time and most vulnerable lines to be hit by attackers.

Furthermore, it is necessary to determine the various backup resource option(s) to aid in restoring the power system and mitigating the impact following an attack. Toward this end, the potential of battery energy storage system (BESS) in enhancing power system resilience attracts the attention. In December 2017, when the Victoria coal power plant supplying 560 MW tripped in Australia, a BESS located 621 miles away stabilized the power grid until proper shutdown, by injecting 7 MW within a few milliseconds [17]. Earlier publications on BESS for power systems have reported several benefits including cost savings [18], integrated electricity-gas system upgrade [19], and T&D upgrade deferral [20]. However, the role of BESS in enhancing the system resilience by functioning as a dispatchable and fast-acting energy resource, especially against malicious attacks, has been rarely discussed. Therefore, the BESS operation has been incorporated in the proposed model to study its effects on unserved energy mitigation when the system encounters malicious attacks. It should be noted that the proposed model aims at minimizing the unserved energy with disabled lines due to attacks. Specific attack tactics, whether physical or cyber, are not distinguished.

This paper has made the following contributions in modeling and evaluation:

1) A tri-level formulation is proposed to model strategical interactions between the attacker and operator in a 24-hour horizon. Specifically, the upper-level problem represents the behaviors of the operator during normal operation. The attack strategy, which includes attack time and lines to be attacked, is formulated in the middle-level problem. Finally, the lower-level problem is formulated from the standpoint of operator during restoration. It should be noted that very few publications have considered multiple time periods in modeling the gameplay between transmission line attackers and system operators. Furthermore, this paper investigates BESS operation during restoration following a transmission line attack.

2) An evaluation of model performance is presented for various model parameters, including attack budget, generator ramping capability, and BESS integration. Furthermore, advantages of the proposed model are quantified in terms of unserved energy mitigation under attacks as compared with the state-of-the-art techniques.

The reminder of the paper is organized as follows: Section II presents the assumptions, architecture and mathematical formulation of the proposed model. Section III introduces the solution technique based on C&CG method. Numerical studies are conducted in section IV. Finally, conclusions are drawn in section V.

II. PROBLEM FORMULATION

A. ASSUMPTION

In this work, it is assumed that the attackers are rational who are capable of destroying the most important transmission line assets. The attacks on these assets could be accomplished by damaging transmission line suspension insulator or transformer bushings. Furthermore, the control signals from relays to breakers can be intercepted and tampered, which causes nuisance tripping of breakers and the corresponding transmission line is disabled. Aforementioned attack actions generally lead to disabled transmission lines, which are unable to carry electrical energy. This paper only discusses system operation considering potential disabled lines due to the attack while characterizing specific attack tactics, either cyber or physical, is out of scope of this paper. It is also assumed that attackers can attack multiple transmission lines simultaneously at any time in 24-hour horizon. In addition, attackers are rational to choose the best attack time considering restoration duration. Finally, when attacked transmission lines are repaired, the system is assumed to be restored back to normal operation, thus having no unserved energy. The overall timeline with events taking place is illustrated in Fig. 1.

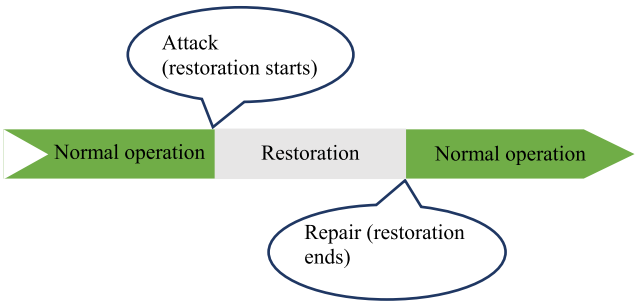

FIGURE 1. Timeline of system status throughout 24 hours.

The operator, from a conservative point of view, seeks to minimize unserved energy during restoration from the attack in the worst-case scenario while reducing operational cost. It is assumed to take same amount of time to repair the attacked lines. The operator also runs the system based on a multi-period DC optimal power flow (DC-OPF) model.

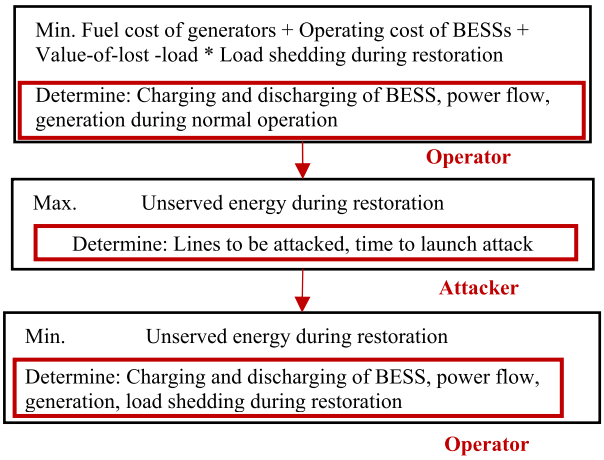

FIGURE 2. Proposed model architecture for minimizing unserved energy under worst scenario with attacks on transmission lines.

B. MODEL ARCHITECTURE

In this section, a tri-level optimization problem is formulated to model interactions between players. The model is built from a conservative point of view, thus robust optimization is applied [21], [22]. The upper-level problem models actions of operator during normal operation. An operator seeks to minimize generation fuel costs, BESS operating costs, and loss-of-load costs during potential restoration from attacks, subject to constraints in a multi-period DC-OPF model. The middle-level problem models the behavior of attacker whose goal is to maximize unserved energy by disabling the transmission lines. Decision variables for the attacker include lines to be attacked and attack time. Lower-level problem represents the response of operator following the attack. The operator redispatches the system to minimize unserved energy before they repair attacked lines. The sequence in the game is to have the player in the higher level make decisions at first. Consequently, variables in higher level problems become constants in lower level problems. All three levels are thus coupled. In specific, the upper-level problem and the lower-level problem are coupled with ramp limits for generators dispatch during normal operation and during restoration. Moreover, initial stored energy in BESS during restoration is determined during normal operation stage. The effects of attacked lines and attack time on system redispatch during restoration show couplings between the middle-level and the lower-level problem. Fig. 2 illustrates the architecture of the proposed model.

C. MATHEMATICAL FORMULATION

$$\underset{\Xi 1}{Minimize} \quad \sum_{t=1}^{T}\sum_{i=1}^{I} FC_{i,t} + \sum_{t=1}^{T}\sum_{b=1}^{B} w * (Pd_{b,t} + Pc_{b,t}) + Voll * \sum_{t=1}^{T}\sum_{n=1}^{N} (Lshc_{n,t} * x_t) \tag{1}$$

$$\text{Subject to} \quad \sum_{i\epsilon\Omega_n^I} P_{i,t} + \sum_{b\in\Omega_n^B}\left(Pd_{b,t} * \eta b - \frac{Pc_{b,t}}{\eta b}\right) + \sum_{l|D(l)=n} Pf_{l,t} - \sum_{l|O(l)=n} Pf_{l,t} = Lo_{n,t}, \quad \forall n, t \tag{2}$$

$$0 \le P_{i,t} \le P_i^{\max}, \quad \forall i, t \tag{3}$$

$$-RD_i \le P_{i,t+1} - P_{i,t} \le RU_i, \quad \forall i, t \tag{4}$$

$$FC_{i,t} = f\left(a_i * P_{i,t}^2 + b_i * P_{i,t} + c_i\right), \quad \forall i, t \tag{5}$$

$$SoC^{\min} * EB_b \le RC_{b,t} \le SoC^{\max} * EB_b, \quad \forall b, t \tag{6}$$

$$RC_{b,t+1} = RC_{b,t} - Pd_{b,t+1} + Pc_{b,t+1}, \quad \forall b, t \tag{7}$$

$$0 \le Pd_{b,t} \le PB_b, \quad \forall b, t \tag{8}$$

$$0 \le Pc_{b,t} \le PB_b, \quad \forall b, t \tag{9}$$

$$RC_{b,t1} = RC_{b,t24}, \quad \forall b \tag{10}$$

$$-Pf_l^{\max} \le Pf_{l,t} \le Pf_l^{\max}, \quad \forall n, t \tag{11}$$

$$B_l * \left(\theta_{n|E(n)=l,t} - \theta_{n|I(n)=l,t}\right) = Pf_{l,t}, \quad \forall l, t \tag{12}$$

Where $\Xi 1 = \{P_{i,t}, Pd_{b,t}, Pc_{b,t}, RC_{b,t}, Pf_{l,t}, \theta_{n,t}, Lsh_{n,t}\}$.

The upper-level problem is formulated in (1)−(12). The objective function, as shown in (1), minimizes the fuel costs of the generators, BESSs operating costs, and loss-of-load cost during restoration. Specifically, the terms, $\sum_{t=1}^{T}\sum_{i=1}^{I} FC_{i,t}$ and $\sum_{t=1}^{T}\sum_{b=1}^{B} w * (Pd_{b,t} + Pc_{b,t})$, calculate generators fuel costs and operating costs of BESSs, respectively. The term, $Voll * \sum_{t=1}^{T}\sum_{n=1}^{N} (Lshc_{n,t} * x_t)$, represents loss-of-load cost during restoration. Deep charging and discharging batteries are penalized by a degradation weighting factor w. In this paper, it is assumed that securing the energy delivery has the highest priority in the system operation. Therefore, the value of lost-loads (*Voll*) is set sufficiently high. Constraint (2) enforces the nodal power balance equations. Constraint (3) imposes bounds on power outputs from generators, and constraint (4) represents ramping up and ramping down limits of generators. The relationship between fuel cost and power outputs of generators is indicated by constraint (5). Fuel cost is obtained by piecewise linearization of a quadratic function, which is approximated with 3 segments. Stored energy limits of BESSs are formulated in (6), and energy balance equations of BESSs are represented by (7). Constraints (8) and (9) enforce limits on charging and discharging power of BESSs. Constraint (10) implies that stored energy in BESS at the end of a day must return to stored energy at the beginning of the day to reach an energy neutral position. Constraint (11) imposes limits on power flow of each line that is calculated by (12).

$$\underset{a_l, x_t, y_t, z_t}{Maximize} \quad \sum_{t=1}^{T}\sum_{n=1}^{N} Lshc_{n,t} * x_t \tag{13}$$

$$\text{Subject to} \quad \sum_{l=1}^{L} a_l \le A^{\max} \tag{14}$$

$$x_{t+1} - x_t = y_{t+1} - z_{t+1}, \quad \forall t \tag{15}$$

$$\sum_{t=1}^{T} y_t = 1 \tag{16}$$

$$\sum_{t=1}^{T} z_t = 1 \tag{17}$$

$$\sum_{t=1}^{T} y_t * z_{t+AD} = 1 \tag{18}$$

$$(a_l, x_t, y_t, z_t) \in (1, 0) \tag{19}$$

The middle-level problem is formulated in (13)−(19). The objective function, shown in (13), maximizes the unserved energy during restoration process. The binary variable x_t stands for the system status. When $x_t = 1$, the system is in restoration process, when $x_t = 0$, the system is in normal operation. Constraint (14) indicates that attacker cannot attack more than $A^{\max}$ lines. Constraint (15) represents the transit of system status (x_t) that is determined by restoration starting indicator (y_t) and ending indicator (z_t). This is similar to the logic of turn on/turn off operation of generators in unit commitment model [23]. Constraints (16) and (17) imply that only one attack happens in 24 hours. Constraint (18) guarantees that restoration process lasts for *AD* hours. All the variables in the middle-level problem are binary variables as shown in (19).

$$\underset{\Xi 1}{Minimize} \quad \sum_{t=1}^{T} \sum_{n=1}^{N} Lshc_{n,t} * x_t \tag{20}$$

$$\text{Subject to } \Big(\sum_{i \in \Omega_n^I} P_{i,t} + \sum_{b \in \Omega_n^B} \left(Pdc_{b,t} * \eta b - \frac{Pcc_{b,t}}{\eta b}\right) + \sum_{l|D(l)=n} Pfc_{l,t} - \sum_{l|O(l)=n} Pfc_{l,t} + Lshc_{n,t}\Big) * x_t = Lo_{n,t} * x_t, \quad \forall n, t(\pi_{n,t}) \tag{21}$$

$$0 \le Pc_{i,t} * x_t \le P_i^{\max} * x_t, \quad \forall i, \in T \left(\alpha_{i,t}^{\max} \alpha_{i,t}^{\min}\right) \tag{22}$$

$$-RD_i * x_t \le \left(Pc_{i,t+1} - Pc_{i,t}\right) * x_t \le RU_i * x_t, \quad \forall i, t(\beta_{i,t}^{\max} \beta_{i,t}^{\min}) \tag{23}$$

$$-RD_i * y_t \le \left(Pc_{i,t} - P_{i,t-1}\right) * y_t \le RU_i * y_t, \quad \forall i, t \left(\beta i_{i,t}^{max} \beta i_{i,t}^{min}\right) \tag{24}$$

$$SoC^{\min} * EB_b * x_t \le RCc_{b,t} * x_t \le SoC^{\max} * EB_b * x_t, \quad \forall b, t \left(\delta_{b,t}^{\max} \delta_{b,t}^{\min}\right) \tag{25}$$

$$RCc_{b,t+1} * x_t = \left(RCc_{b,t} - Pdc_{b,t+1} + Pcc_{b,t+1}\right) * x_t, \quad \forall b, t(\mu_{b,t}) \tag{26}$$

$$y_t * \left(RCc_{b,t} - RC_{b,t-1} + Pdc_{b,t} - Pcc_{b,t}\right) = 0, \quad \forall b, t \quad (\mu i_{b,t}) \tag{27}$$

$$0 \le Pdc_{b,t} * x_t \le PB_b * x_t, \quad \forall b, t(\tau_{b,t}^{\max}, \tau_{b,t}^{\min}) \tag{28}$$

$$0 \le Pcc_{b,t} * x_t \le PB_b * x_t, \quad \forall b, t \quad (\$_{b,t}^{\max}, \$_{b,t}^{\min}) \tag{29}$$

$$-Pf_l^{\max} * x_t \le Pfc_{l,t} * x_t \le Pf_l^{\max} * x_t, \quad \forall l, t(\sigma_{l,t}^{\max} \sigma_{l,t}^{\min}) \tag{30}$$

$$B_l * (1 - a_l) * \left(\theta c_{n|E(n)=l,t} - \theta c_{n|I(n)=l,t}\right) * x_t = Pfc_{l,t} * x_t, \quad \forall l, t(€_{l,t}) \tag{31}$$

$$0 \le Lshc_{n,t} * x_t \le Lo_{n,t} * x_t, \quad \forall n, t(\gamma_{n,t}^{\max}, \gamma_{n,t}^{\min}) \tag{32}$$

where $\Xi 2 = \{Pc_{i,t}, Pdc_{b,t}, Pcc_{b,t}, RCc_{b,t}, Pfc_{l,t}, \theta c_{n,t}, Lshc_{n,t}\}$.

The lower-level problem is formulated in (20)−(32). The objective function, shown in (20), minimizes unserved energy during restoration. It should be noted that only the load shedding during restoration is considered ($x_t = 1$) in (20), since no load shedding during normal operation ($x_t = 0$) as stated earlier. Equation (21) gives the nodal power balance constraint during restoration ($x_t = 1$). During normal operation ($x_t = 0$), both sides of the equation are enforced to zero, so nodal power balance constraint no longer holds. Therefore, equation (21) only represents such constraint during restoration ($x_t = 1$). Same logic applies to following constraints. Constraints (22) and (23) impose power output limits and ramping limits of generators during restoration. Constraint (24) enforces limits on generator power outputs at the first hour of restoration due to the ramping limit. Such a limit is valid only at the beginning of restoration ($y_t = 1$). This constraint reveals that generators power outputs at the first hour of restoration period rely on the generators scheduling during normal operation. Constraint (25) imposes limits of stored energy of BESSs during restoration. Equation (26) represents the energy balance of BESSs during restoration. Initial stored energy of BESSs during the restoration are determined by BESSs scheduling during normal operation, as shown in (27) that further shows effects of normal operation on unserved energy during restoration. Constraints (28)−(29) indicate charging and discharging limits of BESSs during restoration. Constraint (30) denotes limits of power flow of each line, which is calculated by (31). The power flow equation (31) incorporates the impact of attacker variable (a_l) which enforces power flow to be zero once attacked ($a_l = 1$). Constraint (32) imposes limits of load shedding during restoration.

As discussed earlier, different levels of the proposed model are linked. In specific, variables in higher level problems are parameters for lower level problems. The link between the middle-level problem and the lower-level problem gets reflected on the objective function and all constraints of the lower-level problem. Except constraints (24) and (27), other expressions in the lower-level problem depend on system status (x_t), while constraints (24) and (27) depend on restoration start indicator (y_t). Furthermore, constraint (31) also relies on attacked lines (a_l). All of those values are decided by the attacker based on the middle-level problem. Constraints (24) and (27) shows the coupling between upper-level problem and lower-level problem. Values of $P_{i,t-1}$ and $RC_{b,t-1}$ in (24) and (27) are constants, determined in the upper-level problem. It can be seen that the upper-level problem is a mixed integer linear programming (MILP), the middle-level problem is an integer programming, and the lower-level problem is a linear programming (LP).

III. SOLUTION TECHNIQUE

To solve the proposed tri-level model, strong duality theorem [24] together with C&CG method are applied.

$$\left(\sum\nolimits_{n\epsilon\Omega_i^N}\pi_{n,t}+\alpha_{i,t}^{\max}-\alpha_{i,t}^{\min}\right)*x_t - \left(\beta_{i,t}^{\max}-\beta_{i,t}^{\min}-\beta_{i,t-1}^{\max}+\beta_{i,t-1}^{\min}\right)*x_t + \left(\beta i_{i,t}^{\max}-\beta i_{i,t}^{\min}\right)*y_t=0,\quad \forall i,t \tag{33}$$

$$(\eta b*\sum\nolimits_{n\epsilon\Omega_b^N}\pi_{n,t}+\tau_{b,t}^{\max}-\tau_{b,t}^{\min}+\mu_{b,t-1})*x_{t-1} + \mu i_{b,t}*y_t=0,\quad \forall b,t \tag{34}$$

$$(-\sum\nolimits_{n\epsilon\Omega_b^N}\frac{\pi_{n,t}}{\eta b}+£_{b,t}^{\max}-£_{b,t}^{\min}-\mu_{b,t-1})*x_{t-1} - \mu i_{b,t}*y_t=0,\quad \forall b,t \tag{35}$$

$$(\pi_{l|D(l)=n,t}-\pi_{l|O(l)=n,t}+\sigma_{l,t}^{\max}-\sigma_{l,t}^{\min}-€_{l,t}) *x_t=0,\quad \forall l,t \tag{36}$$

$$x_t*(1+\pi_{n,t}+\gamma_{n,t}^{\max}-\gamma_{n,t}^{\min})=0,\quad \forall n,t \tag{37}$$

$$\left(\delta_{b,t}^{\max}-\delta_{b,t}^{\min}\right)*x_t-\mu_{b,t}*x_t+\mu_{b,t-1} *x_{t-1}+\mu i_{b,t}*y_t=0,\quad \forall b,t \tag{38}$$

$$x_t*(1-a_l)*(B_{l1}*€_{l1,t}-B_{l2}*€_{l2,t})=0,\quad l1=FD\,(n\neq n2),\quad l2=FU\,(n\neq n2),\ \forall t \tag{39}$$

$$\alpha_{i,t}^{\max},\alpha_{i,t}^{\min},\beta_{i,t}^{\max},\beta_{i,t}^{\min},\beta i_{i,t}^{\max},\beta i_{i,t}^{\min}\geq 0,\quad \forall i,t \tag{40}$$

$$\delta_{b,t}^{\max},\delta_{b,t}^{\min},\tau_{b,t}^{\max},\tau_{b,t}^{\min},\$_{b,t}^{\max},\$_{b,t}^{\min}\geq 0,\forall b,t \tag{41}$$

$$\sigma_{l,t}^{\max},\sigma_{l,t}^{\min}\geq 0,\quad \forall l,t \tag{42}$$

$$\gamma_{n,t}^{\max},\gamma_{n,t}^{\min}\geq 0,\quad \forall n,t \tag{43}$$

$$\sum\nolimits_{t=1}^{T}\sum\nolimits_{n=1}^{N}x_t*Lsh_{n,t}=-x_t*\sum\nolimits_{t=1}^{T}\sum\nolimits_{n=1}^{N} \pi_{n,t}*Lo_{n,t}-x_t*\sum\nolimits_{t=1}^{T}\sum\nolimits_{n=1}^{N}P_n^{\max}*\alpha max_{n,t}-x_t *\sum\nolimits_{t=1}^{T}\sum\nolimits_{n=1}^{N}RUP_n*\beta_{n,t}^{\max}-x_t *\sum\nolimits_{t=1}^{T}\sum\nolimits_{n=1}^{N}RDP_n*\beta_{n,t}^{\min}-y_t*\sum\nolimits_{t=1}^{T}\sum\nolimits_{n=1}^{N} \left(RUP_n+P_{n,t-1}\right)*\beta i_n^{\max}-y_t*\sum\nolimits_{t=1}^{T}\sum\nolimits_{n=1}^{N} \left(RDP_n-P_{n,t-1}\right)*\beta i_n^{\min}-\sum\nolimits_{t=1}^{T}\sum\nolimits_{n=1}^{N}SoC^{\max}*EB_n *\delta_{n,t}^{\max}*x_t+\sum\nolimits_{t=1}^{T}\sum\nolimits_{n=1}^{N}SoCc^{\min}*EB_n*\delta_{n,t}^{\min}*x_t - \sum\nolimits_{t=1}^{T}\sum\nolimits_{n=1}^{N}y_t*\mu i_{n,t}*RC_{n,t-1} - \sum\nolimits_{t=1}^{T}\sum\nolimits_{n=1}^{N}x_t*PB_n*\tau_{n,t}^{\max} - \sum\nolimits_{t=1}^{T}\sum\nolimits_{n=1}^{N}x_t*PB_n*\$_{n,t}^{\max} - \sum\nolimits_{t=1}^{T}\sum\nolimits_{l=1}^{L}Pf_l^{\max}*\sigma_{l,t}^{\max}*x_t - \sum\nolimits_{t=1}^{T}\sum\nolimits_{l=1}^{L}Pf_l^{\max}*\sigma_{l,t}^{\min}*x_t - \sum\nolimits_{t=1}^{T}\sum\nolimits_{n=1}^{N}\gamma_{n,t}^{\max}*Lo_{n,t}*x_t \tag{44}$$

A. SUBPROBLEM

The first step is to merge the lower-level problem and middle-level problem into a single-level equivalent. This single-level equivalent serves as the subproblem to identify the worst-case attack strategy. Since the lower-level problem is a LP, it can be exactly replaced by its primal constraints, dual constraints and the strong duality condition. Constraints (21) to (32) are primal constraints, and constraints (33) to (44) formulate dual constraints and the strong duality equality.

Then, the subproblem is formulated as follows:

$$\underset{\Xi 3}{Minimize}\ \sum\nolimits_{t=1}^{T}\sum\nolimits_{n=1}^{N}Lshc_{n,t}*x_t \tag{45}$$

Subject to Primal constraints (14) $\sim$ (19), (21) $\sim$ (32)
Dual constraints (33) $\sim$ (43)
Strong duality equality (44)
where $\Xi 3=\Xi 2\cup\{a_l,x_t,y_t,z_t,\boldsymbol{D}\}$.

Noting that in the subproblem, there exist products of two binary variables, as well as products of a binary variable and a continuous variable. To eliminate the non-linearities, these products of variables need to be linearized. Reference [6] gives detailed linearization method for these bilinear terms, so that the subproblem is equivalent to a MILP.

B. MASTER PROBLEM

After reformulation, the subproblem becomes a non-convex problem. Thus, the strong duality condition no longer holds. We use C&CG method to solve the problem. The master problem is formulated in an abstract form as follows:

$$\underset{S_k,M,O}{Minimize}\ \boldsymbol{C^T}*\boldsymbol{M}-\boldsymbol{G^T}*\boldsymbol{S}+O \tag{46}$$

$$\text{Subject to } O\geq \boldsymbol{G^T}*\boldsymbol{S_k},\forall k\leq K \tag{47}$$

$$\boldsymbol{A_l}*\boldsymbol{S_k}\leq \boldsymbol{C_l},\forall k\leq K \tag{48}$$

$$\boldsymbol{B_l}*\boldsymbol{S_k}=\boldsymbol{D_l},\forall k\leq K \tag{49}$$

$$\boldsymbol{A_u}*\boldsymbol{M}\leq \boldsymbol{C_u} \tag{50}$$

$$\boldsymbol{C_u}*\boldsymbol{M}=\boldsymbol{D_u} \tag{51}$$

The master problem includes variables in both the upper-level problem and the lower-level problem. In addition, variables in the lower-level problem are incorporated with a subscript k, the iteration index. Variables in the middle-level problem are constants passed from solution of subproblem. The auxiliary variable O is used as the cutting-plane to refine the feasible set iteratively. Noting that both master problem and subproblem are MILP problems, so global optimality can be guaranteed using commercial solvers such as CPLEX.

C. ALGORITHM IMPLEMENTATION

The C&CG method is used to solve the reformulated tri-level problem. Specifically, the master problem and subproblem are solved iteratively until the tolerance gap is small enough. The detailed solving procedure is stated as follows:

Step 1: Initialization: Set the upper bound and lower bound to positive infinite and negative infinite (UB $=+\infty$,

LB $= -\infty$). Set the iteration index $k = 1$. Obtain initial values of $P_{i,t}$ and $RC_{b,t}$ by basic multi-period DC-OPF model and pass them to the subproblem.

Step 2: Solve the subproblem with the given values of $P_{i,t}$ and $RC_{b,t}$. Obtain the value of objective function. Update the upper bound as UB=min(UB, $\sum_{t=1}^{T}\sum_{n=1}^{N} Lshc_{n,t} * x_t$). Get the results of variables in the middle-level problem (a_l, x_t, y_t, z_t) and pass them to the master problem.

Step 3: With the given values of a_l, x_t, y_t, and z_t, solve the master problem. Update the lower bound as LB=max(LB, O). If (UB-LB)/LB$\leq$CT, stop; otherwise, obtain the values of $\boldsymbol{P_{i,t}}$ and $\boldsymbol{RC_{b,t}}$ and pass them to subproblem, go to step 2. Fig. 3 illustrates the iteration process flowchart.

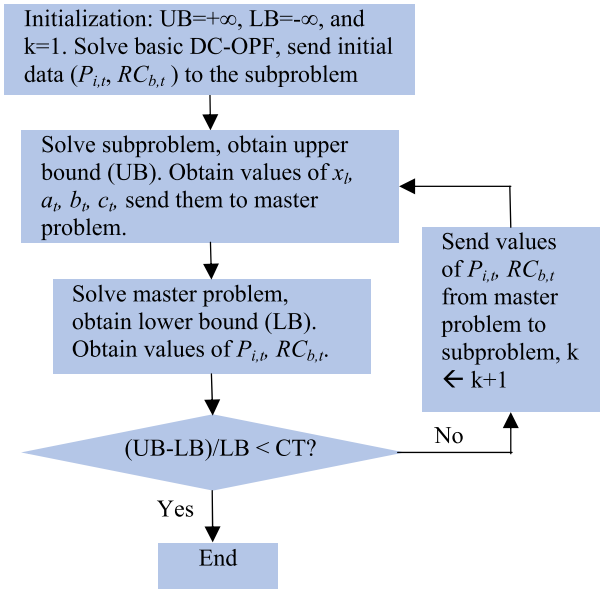

FIGURE 3. Flowchart illustrating the iteration process.

IV. CASE STUDIES

In this section, the performance of proposed model is demonstrated on both Western System Coordinating Council (WSCC) 9-bus and IEEE 57-bus systems. At first, actions of attacker under various settings are tested. Then, a sensitivity analysis is conducted to investigate the impacts of various factors on the amount of unserved energy during restoration. The performance of proposed model on unserved energy reduction is evaluated by comparing with the performance of the basic multi-period DC-OPF model. All the optimization models are implemented in General Algebraic Modeling System (GAMS) using a laptop with an Intel Core i7 CPU and 16 GB RAM. IBM CPLEX is selected as the solver and convergence tolerance is set to 0.1%. For the BESSs, values of initial SoC, maximum SoC, and minimum SoC are assumed to be 0.7, 0.95, and 0.2, respectively. The value of w is assumed to be 0.05, and charging/discharging efficiency of BESSs to 88% [25].

A. WSCC 9-BUS SYSTEM

In the WSCC 9-bus system [24], there are 3 generators, 9 buses and 9 transmission lines. Table I lists the parameters of generators, and the transmission line parameters are provided in [26]. Two equal-rated BESSs for 20 MWh/20 MW are installed on buses #2 and #5. Fig. 4 shows three load profiles having different demand peak hours, corresponding to the historical trend in California during summer [27].

TABLE 1. Generator data in WSCC 9-bus system.

Gen.	Power rating (MW)	Ramping up/down limits (MW)	a_i	b_i	c_i
I1	250	125/250	0.008	13.4	24.4
I2	300	150/300	0.007	23.4	54.2
I3	270	135/270	0.006	28.4	65

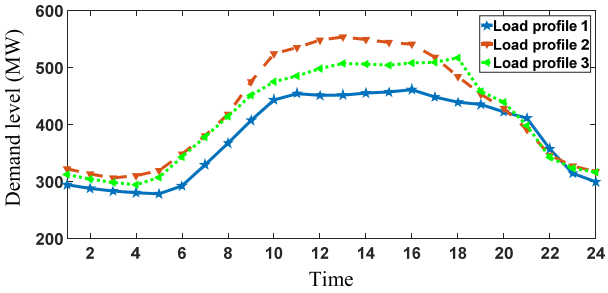

FIGURE 4. Three load profiles of WSCC 9-bus system.

To begin with, actions of attacker and operator during restoration are demonstrated. Then, attack times for different load profiles and restoration durations are obtained. It is assumed that stored energy in BESS1 and BESS2 remain 10 MWh and 12 MWh, respectively, and productions of generators are 50% of their capacity throughout the day. For the assumption that up to 2 lines are attacked, Table II lists attack times for different load profiles and restoration durations. It shows that the optimal attack time varies for different load profiles and restoration durations. The attacked lines and attack times using proposed model for various attack budgets ($A^{\max}$) and restoration durations (AD) are tabulated in Table III, which shows that attack plans vary with attack budgets and restoration durations. For the rest of tests of WSCC 9-bus system, the load profile 1 is deployed since the peak load occurs around 16:00 according to California Independent System Operator (CAISO).

TABLE 2. Attack time for different load profiles and restoration durations in WSCC 9-bus system.

Load profile	AD=2	AD=3	AD=4	AD=5
1	t15	t14	t13	t12
2	t13	t12	t12	t12
3	t17	t16	t15	t14

To illustrate reduced unserved energy by using proposed model, the following two approaches are evaluated:

TABLE 3. Attack lines and times for different attack budgets and restoration durations.

A^{max}	AD=2	AD=3	AD=4
2	*l*4, *l*9, t15	*l*1, *l*4, t12	*l*1, *l*4, t13
3	*l*1, *l*4, *l*9, t15	*l*1, *l*4, *l*9, t14	*l*1, *l*4, *l*9, t13

Approach A: Using proposed model.

Approach B: Using the basic multi-period DC-OPF: Run the basic multi-period DC-OPF model to get the values of $P_{i,t}$ and $RC_{b,t}$. Then, run the subproblem with the obtained values of $P_{i,t}$ and $RC_{b,t}$ to obtain the value of unserved energy.

Fig. 5 shows unserved energy for different attack budgets, restoration durations and approaches. It illustrates that unserved energy is more serious with higher attack budget and longer restoration duration. This is evident as having more disabled lines for longer duration leads to higher unmet demand. Furthermore, a comparison between two approaches for the unserved energy is also shown. It illustrates the benefit of the proposed method in mitigating unserved energy. Another observation is that with more attacked lines, the advantage of the proposed method is less significant. This is because more attacked lines lead to increasing number of islanded generators and BESSs. With less available power sources, the advantage of the proposed method is impaired.

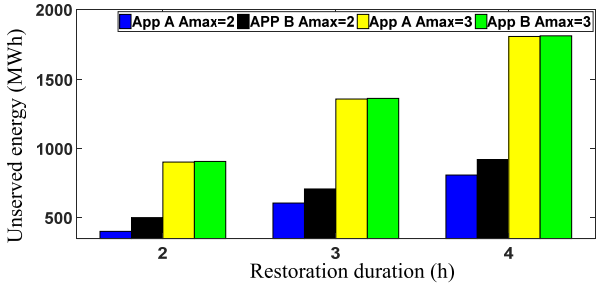

FIGURE 5. Unserved energy for different restoration durations (*AD*), attack budgets (A^{max}) and approaches of WSCC 9-bus system.

B. IEEE 57-BUS SYSTEM

The IEEE 57-bus system is taken from the American Electric Power network. There are 7 generators, 42 loads, 80 lines, and 57 buses. Parameters of generators are tabulated in Table IV and [28] provides additional transmission line parameters. Additionally, four BESSs with capacity of 20MWh/20MW are installed on buses #3, #12, #21, #44. Fig. 6 shows three load profiles in accordance with the historical trends according to CAISO [27].

At first, attack strategies are obtained to demonstrate the subproblem. Assuming stored energy in all BESSs is 10 MWh and generators are producing 50% of total capacity throughout the day, Table V lists the attack times for different load profiles and restoration durations. Like the conclusion in WCSS 9-bus system, the attack time varies with load profiles and restoration durations. For the remainder of test cases of IEEE 57-bus system, load profile 3 is applied whose peak

TABLE 4. Generator data in IEEE 57-bus system.

Gen.	Power rating (MW)	Ramping up/down limits (MW)	a_i	b_i	c_i
I1	575.88	287.94/575.88	0.008	21.7	24.4
I2	100	50/100	0.007	95.2	54.2
I3	140	70/140	0.006	43.4	65
I4	100	50/100	0.004	30.8	35
I5	100	50/100	0.005	99.8	46.2
I6	100	50/100	0.005	97.4	33.1
I7	100	50/100	0.006	46.7	40.8

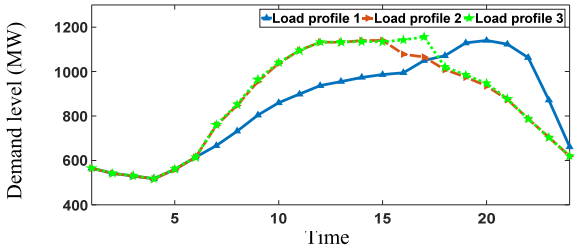

FIGURE 6. Three load profiles of IEEE 57-bus system.

TABLE 5. Attack time for different load profiles and restoration durations in IEEE 57-bus system.

Load profile	AD=2	AD=3	AD=4
1	t20	t19	t19
2	t14	t13	t12
3	t16	t15	t14

load occurs at 16:00 which is normal in California. Table VI presents attack times and attacked lines using proposed model with different attack budgets (A^{max}) and restoration durations (*AD*) for IEEE 57-bus system. Results show that there might be multiple attack strategies lead to the same amount of peak unserved energy. This is because the aim of operator is to minimize unserved energy in the worst-case scenario. In other words, the operator schedules optimally to avoid excessive unserved energy from one specific attack plan. As a result, there might be multiple attack strategies are optimal in terms of maximizing unserved energy.

TABLE 6. Attack lines and times for different attack budgets and restoration durations.

A^{max}	AD=2	AD=3	AD=4
2	*l*17 *l*28 t11 *l*17 *l*28 t12 *l*17 *l*28 t13 *l*15 *l*20 t14 *l*15 *l*18 t15 *l*15 *l*18 t16	*l*15 *l*18 t15	*l*15 *l*18 t14
3	*l*15 *l*18 *l*31 t16	*l*15 *l*19 *l*32 t15	*l*17 *l*20 *l*33 t14
4	*l*3 *l*6 *l*17 *l*21 t11 *l*3 *l*15 *l*17 *l*18 t12 *l*3 *l*15 *l*17 *l*18 t13 *l*3 *l*6 *l*17 *l*21 t14 *l*3 *l*5 *l*6 *l*17 t15 *l*3 *l*15 *l*17 *l*18 t16	*l*3 *l*5 *l*6 *l*17 t12 *l*3 *l*5 *l*6 *l*17 t13 *l*3 *l*6 *l*17 *l*21 t14 *l*3 *l*5 *l*6 *l*17 t15	*l*3 *l*6 *l*17 *l*21 t14

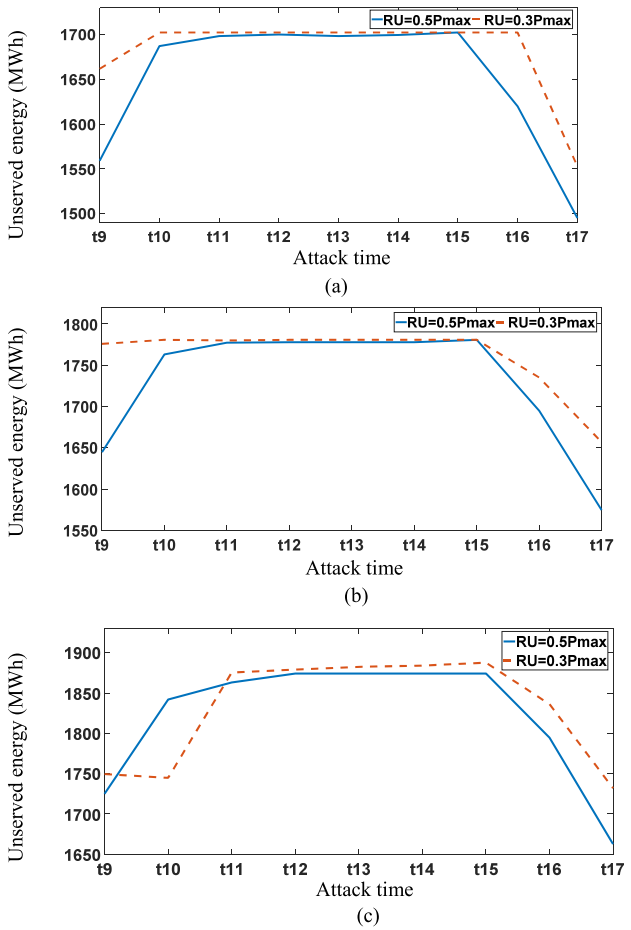

FIGURE 7. Unserved energy for different ramping up limits with AD=3, (a) $A^{\max}$=2, (b) $A^{\max}$=3, (c) $A^{\max}$=4 of IEEE 57-bus system.

Effects of ramping limits on model performance is then discussed. Previous results assume that ramping up limits are 50% of total generation capacity (RU=0.5$P^{\max}$). Fig. 7 shows unserved energy for different ramping up limits with AD=3. As seen in Fig. 7 (a) and (b), for two ramping up limits, unserved energy under the worst-case scenario is the same. However, if RU=0.5$P^{\max}$, only one attack strategy causes the peak value of unserved energy. While if RU=0.3$P^{\max}$, there are 7 and 6 attack strategies lead to maximum unserved energy for $A^{\max}$=2 and $A^{\max}$=3, respectively. When up to 4 lines can be attacked ($A^{\max}$=4), unserved energy in worst case scenario with RU=0.3$P^{\max}$ is larger. Therefore, two conclusions can be drawn from Fig. 7. Firstly, with lower ramping limits, the load curtailment in worst-case scenario will be greater or equal to the scenario with higher ramping limits. It is because lower ramping limits will make generators less flexible to save loads. Secondly, sometimes the application of proposed model might reduce unserved energy after the most serious attack strategy to the case with less tight ramping limits. It further demonstrates value of the proposed model in hedging against the most serious attack strategy.

Finally, the proposed model is compared with the basic DC-OPF strategy in terms of unserved energy under attacks.

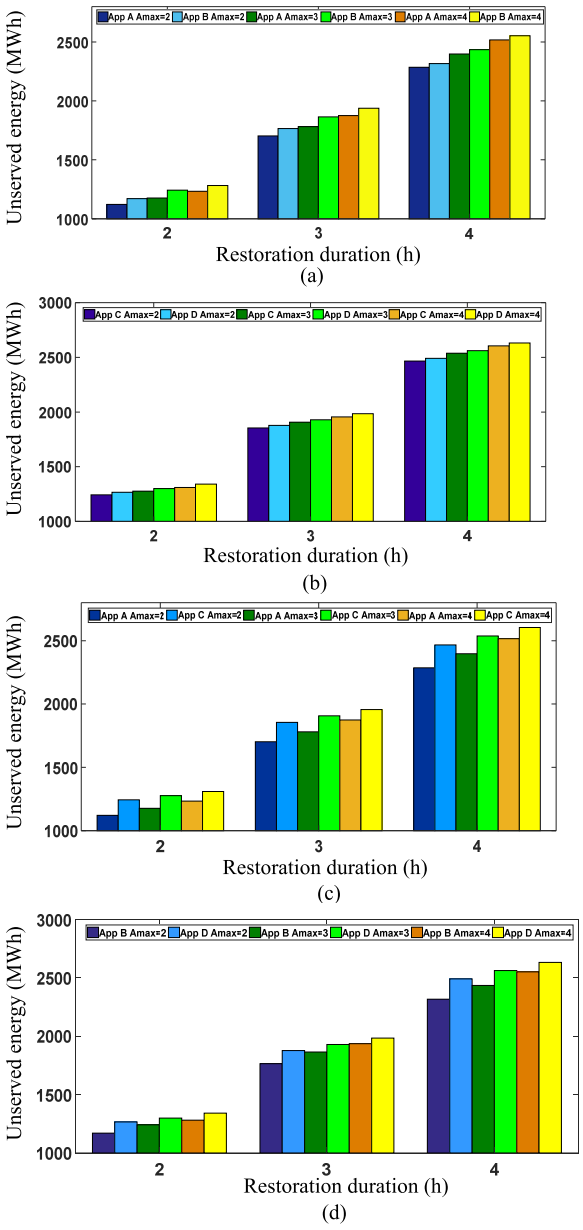

FIGURE 8. Unserved energy for different restoration durations (AD), attack budgets ($A^{\max}$) and approaches of IEEE 57-bus system. Comparison between (a) Approach A and Approach B, (b) Approach C and Approach D, (c) Approach A and Approach C, (d) Approach B and Approach D.

In addition to two approaches (namely approach A and approach B) evaluated for the WSCC 9-bus case, another two approaches are compared for IEEE 57-bus system.

Approach C: Using proposed model in the system without BESS.

Approach D: Using the basic multi-period DC-OPF in the system without BESS. Specifically, run the basic multi-period DC-OPF model for the system without BESS, and get the value of $P_{i,t}$. Then, run the subproblem with the obtained value of $P_{i,t}$ for the system without BESS to obtain the value of unserved energy.

Fig. 8 (a) and (b) depict the unserved energy comparisons between approach A and approach B, as well as approach C

and approach D. The results show that unserved energy is alleviated by using the proposed model. This demonstrates the advantage of the proposed model in unserved energy reduction under the worst-case attack. Fig. 8 (c) shows that using proposed model, the performance is better with BESS which confirms enhanced resilience by BESS integration. Same conclusion can be drawn from Fig. 8 (d). In addition, Fig. 8 reveals that unserved energy is more serious with higher attack budget ($A^{\max}$) and longer restoration duration (AD).

V. CONCLUSION

This paper proposed a tri-level optimization model to mitigate worst-case unserved energy with attacks on transmission lines. The upper-level problem represents actions of operators during normal operation. The attacker determines the attack time and lines to be attacked to maximize unserved energy during restoration in the middle-level problem. The lower-level problem models actions of the operator during restoration. To solve this model, we used strong duality theorem and Column-and-Constraint Generation method.

Two numerical case studies are conducted to demonstrate the proposed model. By comparing unserved energy with attacks in systems run by the proposed model and the basic multi-period DC-OPF, the paper confirms advantage of the proposed model in terms of unserved energy reduction. Moreover, impacts of model parameters, including attack budgets, restoration duration, ramping limits, and BESS integration on model performance are evaluated. It finds that unserved energy can be alleviated with less disabled lines, shorter restoration duration, more flexible generators and BESS integration.

Further research on applying the proposed model to enhance resilience of interdependent systems is planned for future works. In addition, further analysis and design shall be carried out on attacks targeting on other power grid components, such as breakers, relays, substations, etc.

REFERENCES

[1] A. Greenberg. (2017). *Crash Override Malware Took Down Ukraine's Power Grid Last December|WIRED*. [Online]. Available: https://www.wired.com/story/crash-override-malware/

[2] P. W. Parfomak, "Physical security of the U.S. power grid: High-voltage transformer substations," Congressional Res. Service, Washington, DC, USA, Tech. Rep. R43604, 2014, pp. 1–30.

[3] *Attacks on the Electricity Grid_ US Vulnerable to Physical and Cyberthreats*. Accessed: Jan. 6, 2014. [Online]. Available: https://www.cnbc.com/2014/01/03/attacks-on-the-electricity-grid-us-vulnerable-to-physical-and-cyberthreats.html

[4] C. A. Protection, "Followup on western area power administration's critical asset protection," U.S Dept. Energy, Washington, DC, USA, Tech. Rep. DOE-OIG-16-11, 2016.

[5] X. Zhang, K. Tomsovic, and A. Dimitrovski, "Security constrained multi-stage transmission expansion planning considering a continuously variable series reactor," *IEEE Trans. Power Syst.*, vol. 32, no. 6, pp. 4442–4450, Nov. 2017.

[6] J. M. Arroyo, "Bilevel programming applied to power system vulnerability analysis under multiple contingencies," *IET Gener., Transmiss. Distrib.*, vol. 4, no. 2, pp. 178–190, Feb. 2010.

[7] T. Kim, S. J. Wright, D. Bienstock, and S. Harnett, "Analyzing vulnerability of power systems with continuous optimization formulations," *IEEE Trans. Netw. Sci. Eng.*, vol. 3, no. 3, pp. 132–146, Jul./Sep. 2016.

[8] X. Wu and A. J. Conejo, "An efficient tri-level optimization model for electric grid defense planning," *IEEE Trans. Power Syst.*, vol. 32, no. 4, pp. 2984–2994, Jul. 2017.

[9] Y. Lin and Z. Bie, "Tri-level optimal hardening plan for a resilient distribution system considering reconfiguration and DG islanding," *Appl. Energy*, vol. 210, pp. 1266–1279, Jan. 2018.

[10] N. Nezamoddini, S. Mousavian, and M. Erol-Kantarci, "A risk optimization model for enhanced power grid resilience against physical attacks," *Electr. Power Syst. Res.*, vol. 143, pp. 329–338, Feb. 2017.

[11] Y. Xiang and L. Wang, "An improved defender-attacker-defender model for transmission line defense considering offensive resource uncertainties," *IEEE Trans. Smart Grid*, to be published.

[12] H. Nemati, M. A. Latify, and G. R. Yousefi, "Coordinated generation and transmission expansion planning for a power system under physical deliberate attacks," *Int. J. Elect. Power Energy Syst.*, vol. 96, pp. 208–221, Mar. 2018.

[13] A. Moreira, G. Strbac, R. Moreno, A. Street, and I. Konstantelos, "A five-level MILP model for flexible transmission network planning under uncertainty: A min–max regret approach," *IEEE Trans. Power Syst.*, vol. 33, no. 1, pp. 486–501, Jan. 2018.

[14] L. Zhao and B. Zeng, "Vulnerability analysis of power grids with line switching," *IEEE Trans. Power Syst.*, vol. 28, no. 3, pp. 2727–2736, Aug. 2013.

[15] Y. Wen, C. Guo, H. Pandžić, and D. S. Kirschen, "Enhanced security-constrained unit commitment with emerging utility-scale energy storage," *IEEE Trans. Power Syst.*, vol. 31, no. 1, pp. 652–662, Jan. 2016.

[16] A. Moreira, A. Street, and J. M. Arroyo, "Energy and reserve scheduling under correlated nodal demand uncertainty: An adjustable robust optimization approach," *Int. J. Elect. Power Energy Syst.*, vol. 72, pp. 91–98, Jan. 2015.

[17] *Tesla Battery Races to Save Australia Grid from Coal Plant Crash—Injecting 7MW in Milliseconds_Electrek*. Accessed: Dec. 19, 2017. [Online]. Available: https://electrek.co/2017/12/19/tesla-battery-save-australia-grid-from-coal-plant-crash/

[18] B. Xu *et al.*, "Scalable planning for energy storage in energy and reserve markets," *IEEE Trans. Power Syst.*, vol. 32, no. 6, pp. 4515–4527, Nov. 2017.

[19] B. Zhao, A. J. Conejo, and R. Sioshansi, "Using electrical energy storage to mitigate natural gas-supply shortages," *IEEE Trans. Power Syst.*, vol. 33, no. 6, pp. 7076–7086, Nov. 2018.

[20] X. Zhang and A. J. Conejo, "Coordinated investment in transmission and storage systems representing long- and short-term uncertainty," *IEEE Trans. Power Syst.*, vol. 33, no. 6, pp. 7143–7151, Nov. 2018.

[21] H. Zhang, D. Yue, and X. Xie, "Robust optimization for dynamic economic dispatch under wind power uncertainty with different levels of uncertainty budget," *IEEE Access*, vol. 4, pp. 7633–7644, 2016.

[22] Q. Li *et al.*, "Robust optimal reactive power dispatch with feedback and correction against uncertainty of transmission line parameters," *IEEE Access*, vol. 6, pp. 39452–39465, 2018.

[23] B. Zhao, A. J. Conejo, and R. Sioshansi, "Unit commitment under gas-supply uncertainty and gas-price variability," *IEEE Trans. Power Syst.*, vol. 32, no. 3, pp. 2394–2405, May 2017.

[24] S. A. Gabriel, A. J. Conejo, J. D. Fuller, B. F. Hobbs, and C. Ruiz, *Complementarity Modeling in Energy Markets* vol. 180. New York, NY, USA: Springer, 2013.

[25] H. Farzin, M. Fotuhi-Firuzabad, and M. Moeini-Aghtaie, "A stochastic multi-objective framework for optimal scheduling of energy storage systems in microgrids," *IEEE Trans. Smart Grid*, vol. 8, no. 1, pp. 117–127, Jan. 2017.

[26] *IEEE 9-Bus System—Illinois Center for a Smarter Electric Grid (ICSEG)*. Accessed: Jul. 2017. [Online]. Available: http://icseg.iti.illinois.edu/wscc-9-bus-system/

[27] California ISO. *California ISO—Todays Outlook*. Accessed: Jun. 2017. [Online]. Available: http://www.caiso.com/TodaysOutlook/Pages/default.aspx

[28] *IEEE 57-Bus System—Illinois Center for a Smarter Electric Grid (ICSEG)*. Accessed: Aug. 2017. [Online]. Available: http://icseg.iti.illinois.edu/ieee-57-bus-system/

KEXING LAI (S'15) received the B.S. degree in electrical engineering from Central South University, Changsha, China, in 2014. He is currently pursuing the Ph.D. degree in electrical and computer engineering with The Ohio State University, Columbus, OH, USA. He served as an Intern with the PMU and System Analytics Group, GEIRI North America, San Jose, CA, USA, in 2017.

His current research interests include microgrid protection, power system planning and operation, and power system resilience analysis.

YISHEN WANG (S'13–M'17) received the B.S. degree in electrical engineering from Tsinghua University, Beijing, China, in 2011, and the Ph.D. degree in electrical engineering from the University of Washington, Seattle, WA, USA, in 2017.

He is currently a Power System Research Engineer with GEIRI North America, San Jose, CA, USA. His research interests include power system economics and operation, energy storage, microgrids, and PMU data analytics.

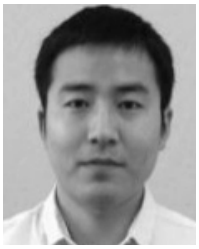

DI SHI (M'12–SM'17) received the Ph.D. degree in electrical engineering from Arizona State University, Tempe, AZ, USA, in 2012.

He currently leads the PMU and System Analytics Group, GEIRI North America, San Jose, CA, USA. He was a Researcher with NEC Laboratories America, Cupertino, CA, USA, and the Electric Power Research Institute, Palo Alto, CA, USA. He served as a Senior/Principal Consultant for eMIT and RM Energy Marketing from 2012 to 2016. He has published over 100 journal and conference papers and holds over 20 U.S. patents/patent applications. He received the IEEE PES General Meeting Best Paper Award in 2017. One energy management and control technology he developed has been commercialized in 2014 into product that helps customers achieve significant energy savings. He is an Editor of the IEEE Transactions on Smart Grid.

MAHESH S. ILLINDALA (S'01–M'06–SM'11) received the B.Tech. degree in electrical engineering from the National Institute of Technology, Calicut, India, in 1995, the M.Sc. (Eng.) degree in electrical engineering from the Indian Institute of Science, Bangalore, India, in 1999, and the Ph.D. degree in electrical engineering from the University of Wisconsin, Madison, WI, USA, in 2005.

Since 2011, he has been a Faculty Member of electrical and computer engineering with The Ohio State University, Columbus, OH, USA. He was a recipient of the 2016 Office of Naval Research Young Investigator Program Award.

His research interests include microgrids, distributed energy resources, electrical energy conversion and storage, power system applications of multiagent systems, protective relaying, and advanced electric drive transportation systems.

XIAOHU ZHANG (S'12–M'17) received the B.S. degree in electrical engineering from the Huazhong University of Science and Technology, Wuhan, China, in 2009, the M.S. degree in electrical engineering from the Royal Institute of Technology, Stockholm, Sweden, in 2011, and the Ph.D. degree in electrical engineering at The University of Tennessee, Knoxville, in 2017.

He is currently a Power System Engineer at GEIRI North America, San Jose, CA, USA. His research interests are power system operation, planning, and stability analysis.

ZHIWEI WANG (M'16–SM'18) received the B.S. and M.S. degrees in electrical engineering from Southeast University, Nanjing, China, in 1988 and 1991, respectively.

He is currently the President of GEIRI North America, San Jose, CA, USA. His research interests include power system operation and control, relay protection, power system planning, and WAMS.